Evaluation of Additive Manufacturing for Wireless Power Transfer Applications

Fabio Corti, *IEEE Membership*, Alberto Reatti, *IEEE Membership*, Luca Pugi, *IEEE Membership*, Gabriele Maria Lozito, *IEEE Membership*, Alicia Triviño-Cabrera, *IEEE Membership*, Leonardo Luchetti and Giacomo Zini

***Abstract*—Additive Manufacturing (AM) has emerged as an economical and feasible technology for creating industrial components. This paper evaluates the use of AM for inductive Wireless Power Transfer (WPT) systems. In particular, the innovative use of metal 3D printing is proposed as a manufacturing process for the coils. For this reason, the recent improvement of metal AM is proposed as a suitable solution to increase design opportunities, reduce costs and production time while improving transmission efficiency. In fact, the WPT coil current distribution can be preliminarily studied through Finite Element Analysis (FEA) to optimize its cross-section and geometry. In this work, a general design procedure for WPT coils using metal AM is presented and this technology is compared with traditional solutions (i.e. hollow and litz wire) through extensive experimental measurements. The analysis shows that AM allows to reduce the parasitic resistance, costs and weight while increasing the transmission efficiency. Thus, the obtained results confirm the potential of AM for producing WPT coils, nominating this technology as a flexible, sustainable, and rapid solution for custom WPT coils production.**

***Index Terms*—Additive Manufacturing, Wireless Power Transfer, Skin Effect, Proximity Effect, Optimization.**

I. Introduction

ADDITIVE Manufacturing is a 3D printing process used to build parts layer by layer, by depositing material according to the design project [1]. This technology has improved significantly in recent years, spreading to many industry sectors, since it allows complex three-dimensional shapes to be generated, difficult to achieve with other approaches. The expansion of this technology has significantly reduced the costs of the printing process. AM generates less waste than traditional manufacturing processes, since it adds material layer by layer, only using the required amount [2]. Finally, the reduced number of steps in the production process leads to energy savings compared to traditional production methods [3]. The reasons described above make AM a flexible, sustainable, and rapid solution for custom parts production [4]. Although polymers are the most commonly used materials, metal and ceramic AM has recently improved, making it available for use in power electronics [5]. Table I shows a literature overview of the main applications related to power electronics. Today, AM is widely used in the field of wearable sensors and ultra-low power far-field energy harvesting [6]- [10]. Another interesting application is the adoption of AM to produce magnetic components. As shown in [11], AM has already been widely tested for inductor production with excellent results. The main advantage of this technique is the possibility to create magnetic core can with a large variety of shapes, optimized for a given specific application [12] [13]. Another promising use is for thermal management. Several studies have proposed optimized heatsink geometries that provide lower thermal resistances and weights than those built with standard techniques [14]- [16]. Finally, AM is widely used for electrical machine manufacturing [17]- [19].

TABLE I
ADDITIVE MANUFACTURING FOR POWER EELECTRONICS: REVIEW

Reference	Application
[6], [7]	Antenna in millimeter wave bands
[8], [9], [10]	Wearables sensors
[11], [12], [13]	Magnetic inductors
[14], [15], [16]	Heatsink
[17], [18], [19]	Electric motors

In this paper, a novel application of AM is investigated. Specifically, the application is oriented to systems made up of coils operating with Alternating Current (AC). For these coils, the winding AC resistance is much higher than the corresponding DC value, due to skin and proximity effects. Thus, operations with high frequency AC lead to a non-uniform distribution of current density in the conductor. The current density is highest near the surface of the conductor and decreases exponentially moving towards the depth of the conductor, leading to higher overall AC resistance. To overcome this problem, two main solutions constitute the state of the art:

- Litz Wire (LW), consisting of many thin wire strands, individually insulated, and twisted together, according to several specific patterns. This strategy equalizes, on average, the length spent at the outside of the conductor for each individual strand, resulting in an equally distributed current in the wire, thus reducing the wire AC resistance.
- Hollow conductor (HC), where part of the internal cross section is removed, making them hollow. This wire makes it possible to save material that would not be used due

to the skin effect. Moreover, some cooling fluid can be injected into the inner part of the conductor section when the applications involve high currents. This solution is more economical than LW, however, the main drawback is the low mechanical strength.

An emerging application where skin and proximity effects strongly affect the system performance is Inductive Wireless Power Transfer (IWPT) [20]- [21]. In these systems, the power is transferred through an airgap by magnetic fields using inductive coupling between two coils. This technology has already been widely used for several applications, ranging from very low-power to high power. Examples of high-power applications are unmanned aerial vehicles [22] and electric vehicle wireless charging [23]- [24]. The latter application is regulated by the IEC 61980 standard [25] and the SAE J2954 guideline [26]. This latter limits the operating frequency to (81.39-90)kHz range. Examples of low-power applications are mobile phone and laptop charging [27]- [28]. These low-power applications are regulated by two main standards: the Qi [29] and the Airfuel [30]. The Qi standard, suggests to operate in the range (110-205) kHz for chargers up to 5 W and (80-300) kHz for chargers up to 120 W. On the other hand, the Airfuel standard suggests an operating frequency of 6.78 MHz.

Due to the high operating frequency, skin and proximity effects strongly affect the conversion efficiency of these systems. In certain cases, the increase in AC resistance is mitigated by using a litz wire. However, this solution is not suitable for all applications: as shown in [31], when operating in the MHz range, the electromagnetic skin depth becomes comparable to (or even smaller than) the smallest strand-diameter available, and it becomes more difficult to obtain a significant benefit from litz wire (i.e. most of manufacturer catalogues trade litz wires capable of operating up to 2.8 MHz [32]- [33]).

This is the motivating factor for this work, which introduces and investigates an innovative use of AM to produce copper conductors with reduced AC resistance and optimized weight. The proposed technique also allows custom-shaped conductors to be printed, which are optimized for a given application. Firstly, the conductor skin and proximity effects are thoroughly investigated using Finite Element Analysis (FEA). With this analysis, the conductor is optimally shaped to minimize its AC resistance, the amount of copper material and its weight.

The performance of conductors resulting from the AM process has been compared with that of litz wire, hollow wire, and solid copper wire. Thus, the main contributions of the paper are summarized as follows:

1) To propose the use of AM as a suitable technology for the realization of WPT coils capable of reducing production costs, speeding up the design process and guaranteeing the designer ample possibilities for creating the most suitable custom geometry.
2) The evaluation and comparison of the AM conductor respect to the traditional technologies which represent the actual state of the art. In particular, a comparison is made against solid copper, hollow copper and litz wire, in terms of current density distribution, AC resistance, weight and cost.

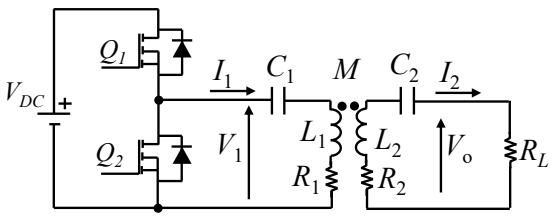

Fig. 1. Power inverter with SS compensation.

3) Experimental evaluation of the transmission efficiency in a WPT workbench using AM planar circular coils tested with the two most common frequencies for IWPT systems (85 kHz and 6.78 MHz), and comparison with the litz wire technology.

The paper is organized as follows. In Section II, the characteristics WPT system are presented and the required inductance is designed to achieve the desired output power.. In Section III, the skin effect on a solid copper wire, hollow wire, litz wire and an AM conductor using FEA simulations is evaluated. The focus has been firstly placed on the cross-section, therefore, a straight conductor of infinite length has been assumed at this stage. Then, the AC resistance per meter for different operating frequencies and the proximity effect has been evaluated to create a circular planar air-cored inductor. In Section IV, some details of the AM process are provided. In Section V, the WPT conversion efficiency using the litz wire, and the AM coil has been experimentally measured. To highlight the advantages of AM, a comparison in terms of weight, costs and performance for the different solutions is provided. Finally, in Section VI the main conclusions and final remarks close the paper.

II. Preliminary Coil Design for IWPT

In an IWPT system, the power is transferred through an airgap between two inductances coupled by a magnetic field. Several coil geometries have been proposed to increase the coupling and make the system less sensitive to misalignment [34]- [35]. In this paper, circular coils are used as a representative geometry, but the following analysis can be simply applied to other cases. As a generic approach, the electrical circuit of a Series-Series (SS) compensation is shown in Fig.1, with R_L equivalent resistance of the rectification stage [36]. The inductances L_1 and L_2 are magnetically coupled and enable the WPT. Resistances in series R_1 and R_2 correspond to the resistances of the primary and secondary coil respectively. These values depend on the operational frequency and the coil design.

The Wheeler formula allows for a first rough estimation of the inductance for a planar circular coil [37]. This formula states:

$$L\,(mH) = 39.37 \cdot 10^{-3} \cdot \frac{a^2 N^2}{8a + 11c} \tag{1}$$

with c = (D_o-D_i)/2 and a = (D_o+D_i)/4 where D_i is the inner diameter and D_o outer diameter. The geometric design of the coils depends on the system constraints. Table II

TABLE II
SYSTEM PARAMETERS AND GEOMETRICAL COIL CHARACTERISTICS

Parameter	Value	Description
V_{DC}	15 V	DC input voltage
P_o	50 W	Output power
D	3 cm	Airgap distance
D_o	10 cm	Outer diameter
N	6	Number of turns
r_W	6	Wire radius
d_W	5 mm	Turns spacing

summarizes the characteristics of the system under study. High values of inductances lead to higher coupling between coils. This can be achieved using the highest possible number of turns N for a given outer diameter, as shown in (1). However, higher number of turns increases the proximity effect, thus leading to higher values of resistance. For this reason, we propose several studies to find a compromise between these two aspects. Using the optimization process shown in [38], the distance between turns d_W and the number of turns N are calculated. The values are shown in Table II.

Substitution of these values in (1) results in L_1=L_2=L=1.5 μH. For simplicity purposes, the two coils are assumed to be identical. Capacitors C_1 and C_2 are tuned to resonate with the inductors L_1 and L_2 at the operating frequency f by using the formula

$$C_1 = C_2 = \frac{1}{\omega^2 L} \tag{2}$$

where $\omega = 2\pi f$.

One of the goals of this work is to evaluate the feasibility of the developed AM technique for most IWPT applications, which work at f_1=85 kHz or at f_2=6.78 MHz. Thus, if the system is designed to operate at f_1, the resonant capacitors are C_1=C_2=2.33μF. On the other hand, when operating at f_2, the required capacitors are C_1=C_2=367pF. In [39], an analytical formulation of the mutual inductance based on the coil geometry is presented. This approach gives a mutual inductance M=0.15 μH obtained at a distance d=3cm. Assuming to operate at the resonant f_2 and neglecting the resistances of the coils, the rms secondary current I_2 is calculated as [40]

$$I_2 = \frac{2}{\pi\sqrt{2}} \frac{V_{DC}}{\omega M} = \frac{V_1}{\omega M} = 1.5A \tag{3}$$

To limit the current density below 4A/mm^2, a wire radius r_W =5mm was selected. In the next section, we evaluate the effect of the skin effect for different cross-sections.

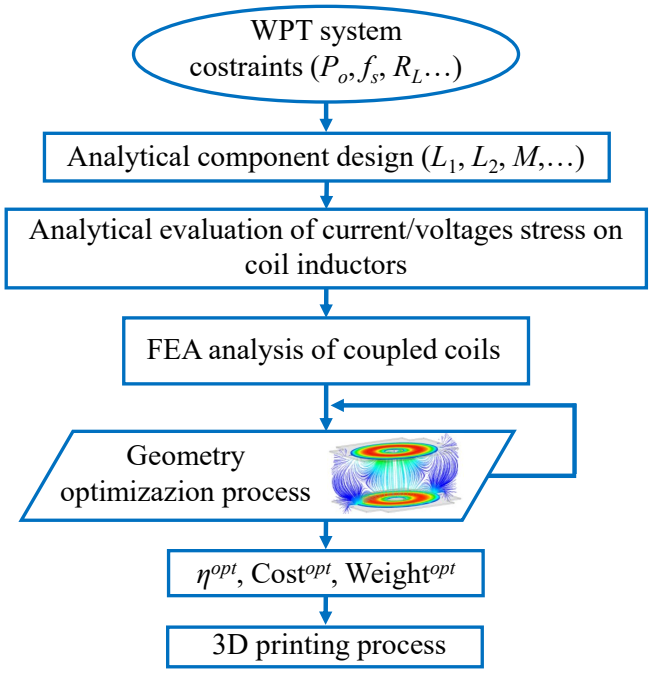

Fig. 2. Flow-chart representation for the coil optimization process.

III. CROSS-SECTION OPTIMIZATION

A flowchart representation of the procedure used for the coil geometry optimization is shown in Fig.2. Starting from a filled conductor, the current distribution due to the skin effect is evaluated and the cross-section of the conductor is iteratively optimized in terms of resistance and weight.

To optimize the cross-section of the coils, it is necessary to understand the main effect that increases its resistance. Skin effect is the tendency of an alternating electric current to be non-uniformly distributed within a conductor, with higher density near the surface and exponentially decreasing towards the depths. The general formula for the skin depth when there is no dielectric or magnetic loss is [41]- [42]:

$$\delta = \sqrt{\frac{2\rho}{\omega\mu}} \sqrt{\sqrt{1 + (\rho\omega\varepsilon)^2} + \rho\omega\varepsilon} \tag{4}$$

where ρ is the conductor material resistivity, $\mu = \mu_0\mu_r$ is the conductor permeability, $\epsilon = \epsilon_0\epsilon_r$ is the permittivity of the conductor and ω=$2\pi f$ is the sinusoidal current angular frequency. The following analysis will be performed assuming a copper material, thus ρ =1.68·$10^{-8}\Omega$m and μ=1.25·10^{-6}H/m. At frequencies $f \ll 1/(\rho\epsilon)$ the quantity inside the large radical is close to unity and (4) reduces to:

$$\delta = \sqrt{\frac{2\rho}{\omega\mu}} \tag{5}$$

In the following, the skin effect in four types of wires is studied: (a) filled conductor, (b) hollow conductor, (c) Litz wire, and (d) additive manufactured wire.

A. Filled Conductor

Using the equation (4), the skin depth in the copper at f_1=85kHz is δ=2.23 mm, while at f_2=6.78MHz is δ=25 μm.

Thus, by increasing the operating frequency, most of the solid conductor cross-section is not used and can be removed reducing cost and weight. This consideration leads to the hollow conductor approach [42].

B. Hollow Conductor

As previously shown, when a copper filled conductor operates in the MHz range the skin depth δ is significantly reduced. This makes very difficult to practically create a hollow wire with such width (i.e. $\delta = 25\mu$m at f_2=6.78 MHz). In addition, too thin thicknesses make it difficult to create geometries with high bending angles due to local buckling moments [43]. To ensure sufficient mechanical stability, a thickness equal to at least 1/5 of the diameter is suggested [44]. For this reason, the cross-section optimization is performed for f_1, since at this frequency, the skin depth is higher than at f_2. Thus, the cross-section optimized at 85kHz will also operate properly at 6.78MHz. To properly design the hollow wire thickness, the AC resistance R_{AC} at different operating frequencies and for different thicknesses Δ has been first investigated, as shown in Fig.3(a). As can be seen, there is an optimum width Δ^* which allows the AC resistance to be minimized depending on the operating frequency. The case at 85 kHz is shown in Fig. 3(b), where an optimum width Δ^*=0.345 mm is required to obtain R_{AC}=4.72mΩ . The interesting aspect is that the ratio between the optimum thickness Δ^* and the skin depth δ is approximately constant over the frequency range analyzed in this paper and equal to $\Delta^*/\delta=\pi/2$, as shown in Fig. 3(c). The current distribution for the optimized hollow cross section at 85 kHz is shown in Fig. 4(a).

C. Litz Wire

Another technology widely used to reduce the skin effect is litz wire. Depending on the operating frequency, strands with different diameters must be used. The number of strands depends on the current flowing through the conductor. Litz wire is a suitable solution when operating in the hundreds of kHz, although it becomes impractical in the MHz range since the width of the strands needs to be extremely thin. This increases the complexity of the production process and costs. Since each litz wire is optimized to operate at a particular frequency, a litz wire made up of 12640 strands AWG 38 has been used to operate at $f_1 = 85$kHz, while a litz wire made up of 26020 strands AWG 48 has been used to operate at $f_2 = 6.78$MHz.

D. Additive Manufactured Wire

The geometries that can be created with AM strongly depend on the characteristics of the 3D printer. Since each layer must be placed on a previously deposed layer, it is not possible to create circular cross-sections unless using appropriate supports, which will increase the production process complexity and costs. For this reason, as shown in Fig.5, angles higher than 50° and a minimum width of 0.5mm are required.

To minimize the copper material, the pentagonal cross-section has been identified. Multiple FEA have been performed

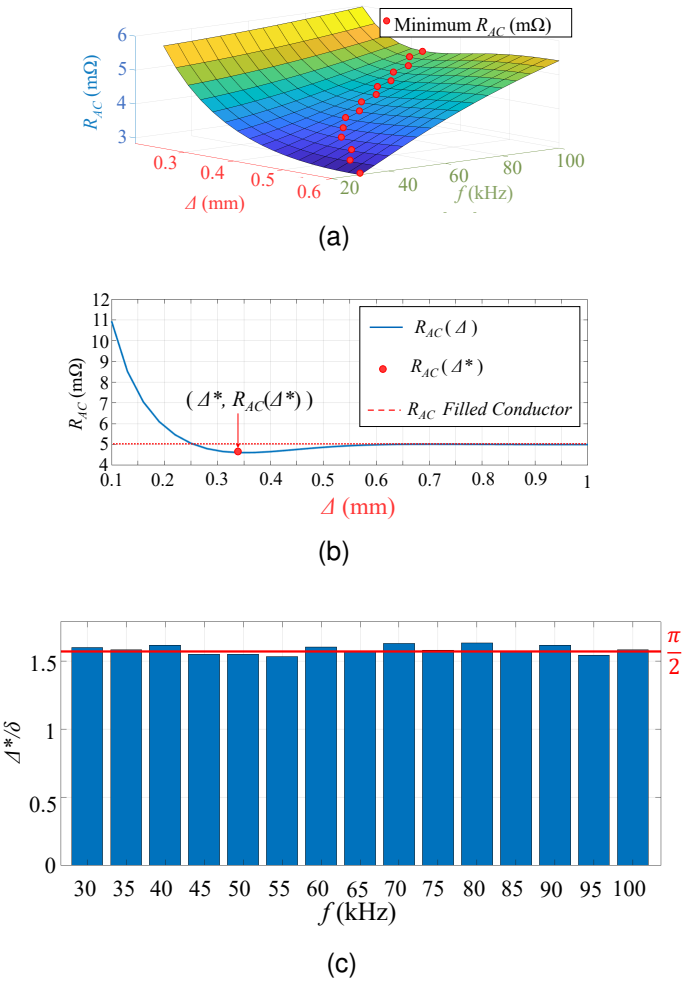

Fig. 3. Hollow wire FEA. (a) AC resistance for different hollow cross-section width Δ and frequency f. (b) Analysis of AC resistance under cross-section variation Δ at 85 kHz. (c) Ratio between hollow depth and skin depth at different frequencies.

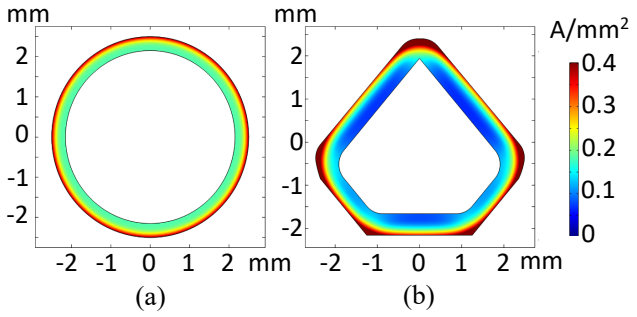

Fig. 4. Current density distribution at 85 kHz. (a) Hollow wire at (b) AM wire.

to identify this geometry as the best compromise between geometry constraints due to the 3D printer characteristics, optimization of the cross-section in terms of saving material and low AC resistance. The current density distribution at 85kHz is shown in Fig.4(b).

The previous analysis was carried out assuming a straight conductor of infinite length since the focus was on the skin effect. Another phenomenon that strongly affects the

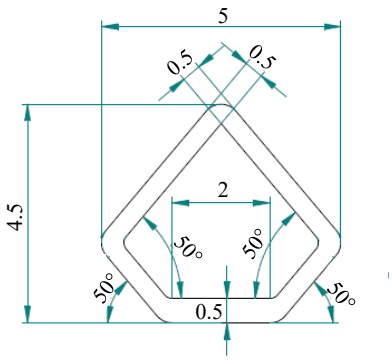

Fig. 5. Pentagonal cross-section derived from the minimum angle and width for the 3D printer constraints. All the dimensions are in millimeters.

equivalent AC resistance of a conductor is the proximity effect. If currents are flowing through one or more other nearby conductors, the current distribution within the first conductor will be constrained to smaller regions. This effect is particularly important in IWPT systems. The current density distribution across the different cross-sections in the $N = 6$ turns of the WPT coils is shown in Fig.6.

The current density on the filled conductors and hollow wire is shown in Fig.6(a) and Fig.6(b) respectively.

The current density across the AM coil is shown in Fig.6(c). As shown, the proximity effect strongly affects the current density distributions on the coils for the three coils considered.

Some conductor areas are also characterized by a very low current density. Based on these results, an additional optimization of the section has been performed, removing the parts that are affected by low current density, as shown in Fig.6(d). This new design with an optimized pentagonal cross-section could generate lighter and cheaper coils. To decide the appropriate value for l_{cut} (Fig.7), further analysis must be carried out. As shown in Fig.6(c), the current density is low on the top-right face of the pentagonal cross-section for the first inner turns, while on the last turn the current density is low on the top-left face. Thus, iterative FEA to compute the optimum length of cut l_{cut} has been computed to select the optimum cut length that maximizes the following objective function:

$$J = J_1 - J_2 - J_3 = \frac{L_{CUT}}{L} - \frac{S_{CUT}}{S} - \frac{R_{CUT}}{R} \qquad (6)$$

where L_{cut}, S_{CUT} and R_{CUT} are the inductance, the surface area and the equivalent resistance of the coil once the section l_{cut} has been removed. In Fig.7, the three terms are shown for different values of l_{cut}. As can be seen, the cut does not significantly affect the value of the inductance and the equivalent resistance. On the other hand, it reduces the surface area, and therefore, the cost and weight. The performance of this geometry, referred to as optimized pentagonal, will be analyzed experimentally in the following sections. The estimated inductance and resistance obtained at f_1 and f_2 through FEA simulations are summarized in Table III.

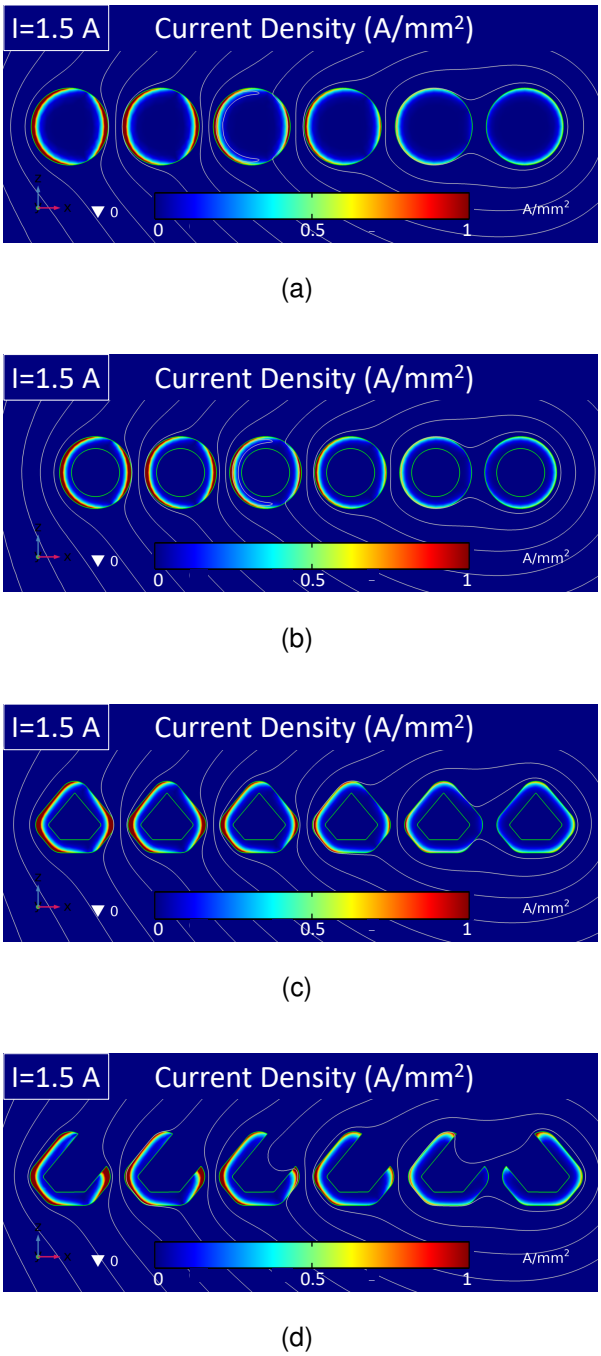

Fig. 6. Proximity effect. (a) Filled wire. (b) Hollow wire. (c) AM wire. (d) Optimized AM wire.

IV. Additive Manufacturing Process

The manufacturing process used to print the coil is called Atomic Diffusion Additive Manufacturing (ADAM)and it has four stages. The first is the design, where the piece is projected and the material is chosen. The second is the construction, where the material, i.e., copper alloy, is deposited through the extruders on the plane. At this point, the piece is about 20% larger than the nominal dimension since it contains wax and polymers, as shown in Fig.8(a). The third stage is the wash, where the wax is removed by solvents such as Opteon SF79. The last stage is the sinter, which is done through a

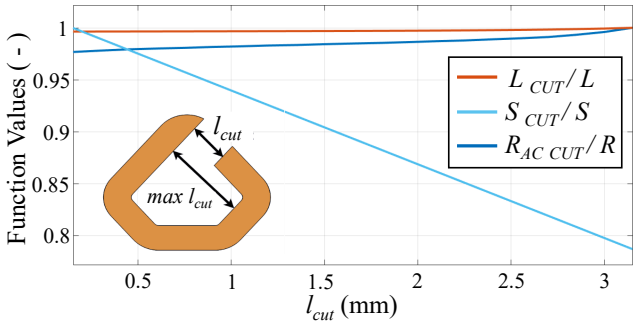

Fig. 7. Analysis of different optimization function contribution for different lengths of cut.

TABLE III
FEA SIMULATED INDUCTANCE AND AC RESISTANCE

Cross-Section	$L(\mu H)$ @85kHz	$R_{AC}(m\Omega)$ @85kHz	$L((\mu H)$ @6.78 MHz	$R_{AC}(m\Omega)$ @6.78MHz
$FilledCopper$	1.77	24.90	1.73	254.0
$Hollow$	1.78	1.39	1.74	253.3
$LitzWire$	1.97	28.49	1.97	3330
$Pentagonal$	1.89	23.86	1.86	237.0
$Opt.Pentagonal$	1.85	24.37	1.81	241.9

combination of temperature and pressure. After this stage, the polymers are eliminated, and the piece is made of metal only. The total cycle can last up to 30 hours. The results of the manufacturing process are presented in Fig.8(b), which shows the optimized coil discussed in the previous section.

V. EXPERIMENTAL RESULTS

In this section, the properties of the AM coils are compared with the other technologies in a particular WPT case study.

A. Frequency Analysis of Additive Manufactured Coil

The impedance magnitude and phase of the coil shown in Fig.9 were evaluated in the range 40 kHz-110 MHz with an impedance analyzer. As can be seen, the coils have similar behavior in terms of frequency. The inductance and the resistance of the coils at the analyzed frequencies are summarized in TableIV. The experimental measurements confirm the results of FEA simulations. The AM wires allow for a lower R_{AC} than litz wire. Moreover, the optimized AM reaches comparable performance in terms of inductance and AC resistance with the AM pentagonal solution but allows for a significant reduction in cost and weight, as we will analyze next.

B. Experimental Setup

To compare the performance of the different coil technologies, the Series-Series compensated WPT circuit shown in Fig.1 has been reproduced experimentally, as shown in Fig.11(b). In particular, the half-bridge inverter consists of a GS66508B-EVBDB1 board including two GaN Enhancement-mode HEMTs GS66508T 650V. The inverter has been driven

(a)

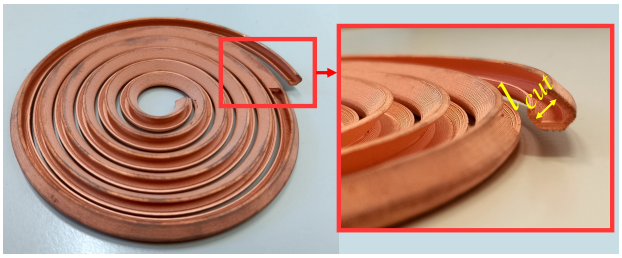

(b)

Fig. 8. Manufactured coils. (a) Fabricated coils, during the construction phase. (b) Detail of the optimized cross-section coil.

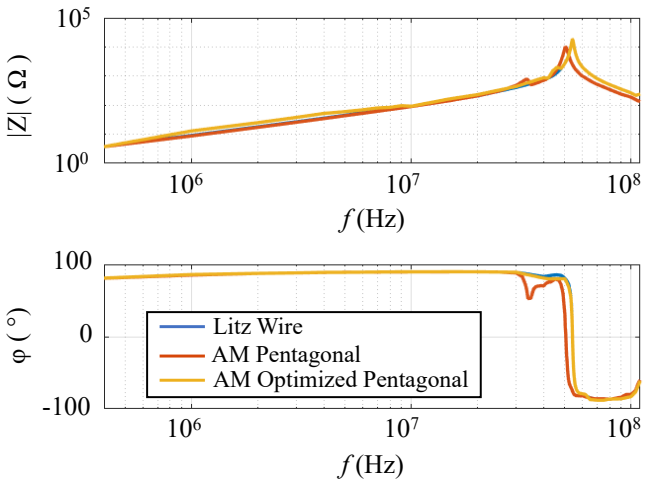

Fig. 9. Measured impedance analysis of different coils.

TABLE IV
MEASURED INDUCTANCE AND AC RESISTANCE

Cross-Section	$L(\mu H)$ @85kHz	$R_{AC}(m\Omega)$ @85kHz	$L(\mu H)$ @6.78 MHz	$R_{AC}(m\Omega)$ @6.78 MHz
$LitzWire$	1.92	28.40	1.97	3278
$Pentagonal$	1.83	21.54	1.89	243
$Opt.Pentagonal$	1.85	23.16	1.87	251

using a STM32 Nucleo H7ZI3Z1, programmed by STM 32

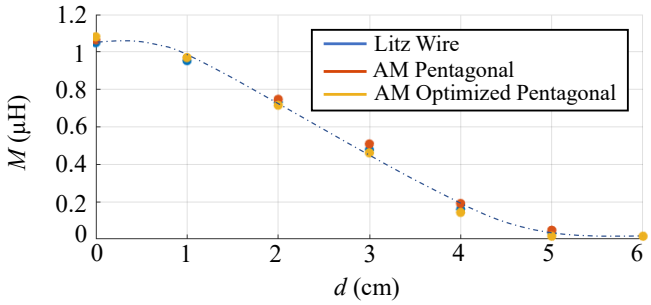

Fig. 10. Measured mutual inductance at different distances for different coil technologies.

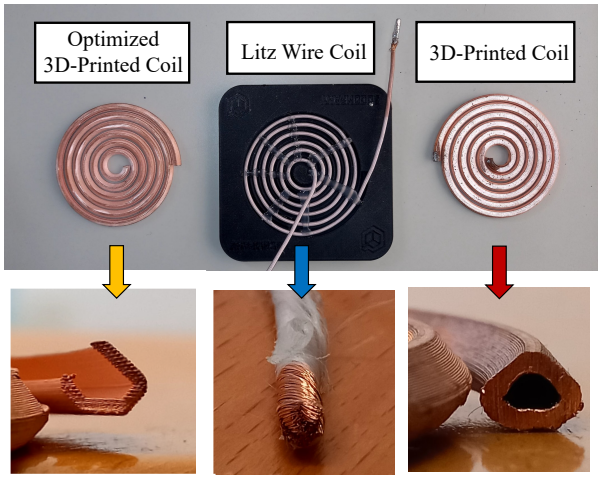

(a)

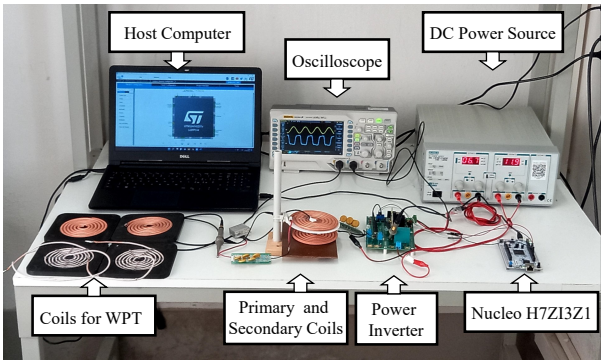

(b)

Fig. 11. Experimental Measurements. (a) Types of coils experimentally analyzed. (b) WPT experimental setup.

Cube IDE. The measured mutual inductance using the three different coils for different distances d is shown in Fig. 10.

The cost related to litz wires depends on the frequency. To operate at $f_1 = 85$kHz, a litz wire made up of 10(5x5x34/38) strands AWG38 has been used, with a cost of approximately 51€/m. To operate at $f_2 = 6.78$MHz, a litz wire made up of 31675 strand AWG 48 has been used, with a cost of approximately 100€/m. Using [45], a length l = 1.28 m for the Archimedean spiral is obtained. Thus, the cost of the coil is

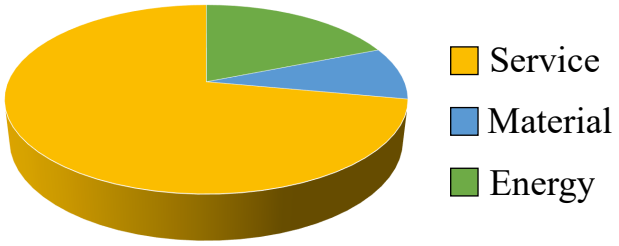

Fig. 12. Cost of metal 3D printing process.

approximately $cost$=65€for the litz operating at $f_1 = 85$kHz and $cost$=128€for the litz operating at $f_2 = 6.78$MHz.

On the other hand, the cost of the AM spiral depends on multiple factors. The four coils (two with pentagonal cross-section and two with optimized pentagonal cross-section) were printed simultaneously, as shown in Fig. 8(a). The time required to produce four coils was approximately 30 hours. The construction stage lasted 8 hours. The power absorbed by the 3D printer during this stage was approximately 1.5 kW. Thus, this stage required 12 kWh. The washing stage lasted 13 hours and the power absorbed by the dryer was approximately 1.65 kW. Thus, this stage required 21.45 kWh. Finally, the sintering stage took 17 hours absorbing approximately 7.2 kW. Thus, this stage required 122.4 kWh. The total amount required was 155.85 kWh. Assuming 0.40€/kWh electricity cost, the energy needed yields 62.34€. The most popular metal 3D printing process, Powder Bed Fusion, involves blasting a powerful laser at a flat bed of powder that instantly creates a tiny melt-pool where the laser focuses. This melt-pool is moved around the bed to gradually build up the solid metal object. Pure copper conducts heat and electricity far more efficiently than traditional metals. Markforged Copper possesses better conductivity characteristics than alloyed copper that can be printed. Approximately 0.5 kg of copper is required to print four coils, leading to a 30€material cost. Finally, service costs amount to approximately 30€/h, totaling 240€. A schematic representation of AM cost is shown in Fig.12. As can be seen, most of the costs related to the metal 3D printing process are related to the service. However, due to increasing demand, the cost of printing processes is going to fall significantly in the coming years, making this technology particularly competitive with traditional coils.

The results of this analysis are summarized Fig. 13(a) and Fig.13(b), where the comparison in terms of transmission efficiency, cost and weight between litz wire and AM coils when the system operate at f_1=85kHz and f_2=6.78MHz are shown repsectively. The main results are:

- The transmission efficiency of AM coil is slightly higher than using litz wire. This The improvement is greater when operating in the MHz range since the advantages deriving from the litz wire are very limited.
- The cost of AM and litz wire is comparable when operating in the kHz range, where a large variety of litz wires are commercially available. On the other hand, the cost associated to litz wire become significantly higher

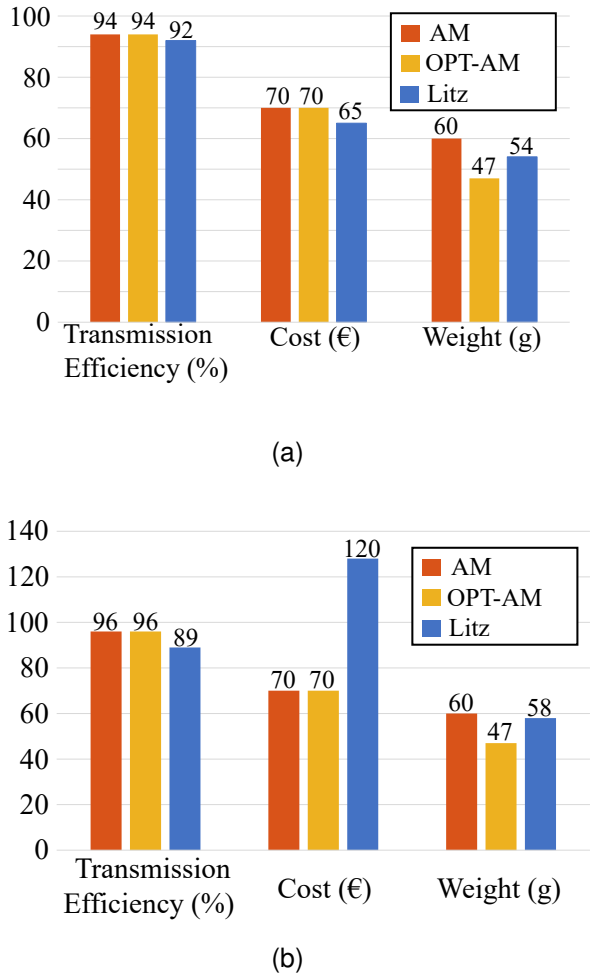

Fig. 13. Comparison of planar circular coil in terms of transmission efficiency, cost and weight. (a) System operating at $f_1 = 85kHz$. (b) System operating at $f_2 = 6.78MHz$.

when operating in the MHz, due to the practical difficulty of making extremely thin strand.

- The weight of AM and litz wire solution are comparable. Through geometry optimization it is possible to reduce the amount of material required for AM, leading to lighter coils.

VI. Conclusions

In this paper, we have presented an innovative application for AM to produce WPT coils. The use of AM allows the creation of a geometry representing the optimal tradeoff between costs and weight. Using FEA software, we first evaluated proximity and the skin effect for different case studies to optimize the cross-section of the conductor, compatibly with the 3D printer constraints. The comparison performed using FEA analysis was validated through experimental results. Finally, a comparison in terms of cost, weight, and performance in WPT applications has also been evaluated and confirmed with experimental results. The following conclusions were derived from this work:

- The AM for WPT applications makes it possible to reduce waste material with respect to traditional manufacturing processes, using only the required amount of material. For large productions, it allows the manufacturing process time and energy consumption to be reduced, leading to lower costs.
- The AM coils are particularly suitable for an AirFuel WPT system where the operating frequency is in the MHz range and the skin effect sharply increases the resistance. It has been proved that this technology makes it possible to drastically reduce the cost of coils compared to litz wires, increasing transmission efficiency.
- The AM allows for a flexible and rapid design of a custom coil for WPT.

As future development, the design of additive manufactured coil for different WPT topologies and coil geometries will be evaluated.

Acknowledgment

The authors wish to thank 3D COMPANY SRL, for producing the coils and providing support during the design process.

References

[1] D. Espalin, D.W. Muse, E. MacDonald, R.B. Wicker RB, "3D Printing multifunctionality: structures with electronics", *The International Journal of Advanced Manufacturing Technology*, Vol. 72, Nr. 5, pp. 963-978, 2014 May.

[2] M.J. Kim, M.A. Cruz, S. Ye, A.L. Gray, G.L. Smith, N. Lazarus, C.J. Walker, H.H. Sigmarsson, B.J. and Wiley, "One-step electrodeposition of copper on conductive 3D printed objects", *Additive Manufacturing*, 2019 May 1; pp.318-326.

[3] P.F. Flowers, C. Reyes, S. Ye, M.J. Kim, and B.J. Wiley, "3D printing electronic components and circuits with conductive thermoplastic filament", *Additive Manufacturing*, 2017 Dec 1; pp.:156-163.

[4] T. Hou et al., "Design of 3D Wireless Power Transfer System Based on 3D Printed Electronics," in *IEEE Access*, vol. 7, pp. 94793-94805, 2019, doi: 10.1109/ACCESS.2019.2928948.

[5] L. Lopera, R. Rodriguez, M. Yakout, M. Elbestawi and A. Emadi, "Current and Potential Applications of Additive Manufacturing for Power Electronics", *IEEE Open Journal of Power Electronics*, vol. 2, pp. 33-42, 2021, doi: 10.1109/OJPEL.2021.3052541.

[6] M. Ferrando-Rocher, J. I. Herranz-Herruzo, A. Valero-Nogueira and B. Bernardo-Clemente, "Selective Laser Sintering Manufacturing as a Low Cost Alternative for Flat-Panel Antennas in Millimeter-Wave Bands," in *IEEE Access*, vol. 9, pp. 45721-45729, 2021, doi: 10.1109/ACCESS.2021.3067637.

[7] J. Zhu et al., "Additively Manufactured Millimeter-Wave Dual-Band Single-Polarization Shared Aperture Fresnel Zone Plate Metalens Antenna," in *IEEE Transactions on Antennas and Propagation*, vol. 69, no. 10, pp. 6261-6272, Oct. 2021, doi: 10.1109/TAP.2021.3070224.

[8] H. Ota et al., "Application of 3D Printing for Smart Objects with Embedded Electronic Sensors and Systems", *Advanced Materials Technologies*, Wiley, March 2016, https://doi.org/10.1002/admt.201600013.

[9] Y. Dong, X. Min and W. S. Kim, "A 3-D-Printed Integrated PCB-Based Electrochemical Sensor System," in *IEEE Sensors Journal*, vol. 18, no. 7, pp. 2959-2966, April1, 2018, doi: 10.1109/JSEN.2018.2801459.

[10] W. Su, B. S. Cook and M. M. Tentzeris, "Additively Manufactured Microfluidics-Based Peel-and-Replace RF Sensors for Wearable Applications," in *IEEE Transactions on Microwave Theory and Techniques*, vol. 64, no. 6, pp. 1928-1936, June 2016, doi: 10.1109/TMTT.2016.2560177.

[11] [Y. Yan, J. Moss, K. D. T. Ngo, Y. Mei and G. Lu, "Additive Manufacturing of Toroid Inductor for Power Electronics Applications," *IEEE Transactions on Industry Applications*, vol. 53, no. 6, pp. 5709-5714, Nov.-Dec. 2017, doi: 10.1109/TIA.2017.2729504.

[12] C. Ding, S. Lu, L. Liu, K. D. T. Ngo and G. -Q. Lu, "Additive Manufacturing of Hetero-Magnetic Coupled Inductors," *IEEE Transactions on Components, Packaging and Manufacturing Technology*, vol. 11, no. 6, pp. 1028-1034, June 2021, doi: 10.1109/TCPMT.2021.3083179.

[13] L. Liu, T. Ge, K. D. T. Ngo, Y. Mei and G. -Q. Lu, "Ferrite Paste Cured With Ultraviolet Light for Additive Manufacturing of Magnetic Components for Power Electronics," *IEEE Magnetics Letters*, vol. 9, pp. 1-5, 2018, Art no. 5102705, doi: 10.1109/LMAG.2018.2822622.

[14] R. Whitt, D. Huitink, A. Emon, A. Deshpande and F. Luo, "Thermal and Electrical Performance in High-Voltage Power Modules With Nonmetallic Additively Manufactured Impingement Coolers," *IEEE Transactions on Power Electronics*, vol. 36, no. 3, pp. 3192-3199, March 2021, doi: 10.1109/TPEL.2020.3015226.

[15] E. M. Dede, S. N. Joshi, and F. Zhou, "Topology optimization, additive layer manufacturing, and experimental testing of an air-cooled heat sink," *Journal of Mechanichal Design*, vol. 137, no. 11, Oct. 2015, Art. no. 111403.

[16] T. Wu, Z. Wang, B. Ozpineci, M. Chinthavali and S. Campbell, "Automated Heatsink Optimization for Air-Cooled Power Semiconductor Modules," *IEEE Transactions on Power Electronics*, vol. 34, no. 6, pp. 5027-5031, June 2019, doi: 10.1109/TPEL.2018.2881454.

[17] R. Wrobel and B. Mecrow, "A Comprehensive Review of Additive Manufacturing in Construction of Electrical Machines," *IEEE Transactions on Energy Conversion*, vol. 35, no. 2, pp. 1054-1064, June 2020, doi: 10.1109/TEC.2020.2964942.

[18] F. Wu, A. M. EL-Refaie and A. Al-Qarni, "Additively Manufactured Hollow Conductors Integrated With Heat Pipes: Design Tradeoffs and Hardware Demonstration," *IEEE Transactions on Industry Applications*, vol. 57, no. 4, pp. 3632-3642, July-Aug. 2021, doi: 10.1109/TIA.2021.3076423.

[19] N. Simpson, D. J. North, S. M. Collins and P. H. Mellor, "Additive Manufacturing of Shaped Profile Windings for Minimal AC Loss in Electrical Machines," *IEEE Transactions on Industry Applications*, vol. 56, no. 3, pp. 2510-2519, May-June 2020, doi: 10.1109/TIA.2020.2975763.

[20] S. H. Lee and R. D. Lorenz, "Development and Validation of Model for 95%-Efficiency 220-W Wireless Power Transfer Over a 30-cm Air Gap," *IEEE Transactions on Industry Applications*, vol. 47, no. 6, pp. 2495-2504, Nov.-Dec. 2011, doi: 10.1109/TIA.2011.2168555.

[21] Q. Deng et al., "Frequency-Dependent Resistance of Litz-Wire Square Solenoid Coils and Quality Factor Optimization for Wireless Power Transfer," *IEEE Transactions on Industrial Electronics*, vol. 63, no. 5, pp. 2825-2837, May 2016, doi: 10.1109/TIE.2016.2518126.

[22] S. Wu, C. Cai, L. Jiang, J. Li and S. Yang, "Unmanned Aerial Vehicle Wireless Charging System With Orthogonal Magnetic Structure and Position Correction Aid Device," *IEEE Transactions on Power Electronics*, vol. 36, no. 7, pp. 7564-7575, July 2021, doi: 10.1109/TPEL.2020.3047384.

[23] O. C. Onar, M. Chinthavali, S. L. Campbell, L. E. Seiber and C. P. White, "Vehicular Integration of Wireless Power Transfer Systems and Hardware Interoperability Case Studies," *IEEE Transactions on Industry Applications*, vol. 55, no. 5, pp. 5223-5234, Sept.-Oct. 2019, doi: 10.1109/TIA.2019.2928482.

[24] G. Yang et al., "Interoperability Improvement for Rectangular Pad and DD Pad of Wireless Electric Vehicle Charging System Based on Adaptive Position Adjustment," *IEEE Transactions on Industry Applications*, vol. 57, no. 3, pp. 2613-2624, May-June 2021, doi: 10.1109/TIA.2021.3056639.

[25] IEC 61980-1:2020 , "Electric vehicle wireless power transfer (WPT) systems - Part 1: General requirements", Available online at: https://webstore.iec.ch/publication/31657.

[26] Standard SAEJ2954. A Wireless Power Transfer for Light-Duty Plug-In/Electric Vehicles and Alignment Methodology. Available online: https://www.sae.org/standards/content/j2954˙201605/ (accessed on 10 December 2020).

[27] T. Feng, Y. Sun, Y. Feng and X. Dai, "A Tripolar Plane-Type Transmitter for Three-Dimensional Omnidirectional Wireless Power Transfer," *IEEE Transactions on Industry Applications*, vol. 58, no. 1, pp. 1254-1267, Jan.-Feb. 2022, doi: 10.1109/TIA.2021.3107471.

[28] M. Huang, Y. Lu and R. P. Martins, "A Reconfigurable Bidirectional Wireless Power Transceiver for Battery-to-Battery Wireless Charging," *IEEE Transactions on Power Electronics*, vol. 34, no. 8, pp. 7745-7753, Aug. 2019, doi: 10.1109/TPEL.2018.2881285.

[29] Standard Qi. Available online: https://qi-wireless-charging.net/

[30] Standard Airfuel. Available online: https://airfuel.org/.

[31] B. A. Reese and C. R. Sullivan, "Litz wire in the MHz range: Modeling and improved designs," 2017 IEEE 18th Workshop on Control and Modeling for Power Electronics (COMPEL), 2017, pp. 1-8, doi: 10.1109/COMPEL.2017.8013391.

[32] New England Wire Catalogue. Available online: https://www.newenglandwire.com

[33] MWS Catalogue. Available online: https://mwswire.com/

[34] F. J. López-Alcolea, J. V. d. Real, P. Roncero-Sánchez and A. P. Torres, "Modeling of a Magnetic Coupler Based on Single- and Double-Layered Rectangular Planar Coils With In-Plane Misalignment for Wireless Power Transfer," *IEEE Transactions on Power Electronics*, vol. 35, no. 5, pp. 5102-5121, May 2020, doi: 10.1109/TPEL.2019.2944194.

[35] I. U. Castillo-Zamora, P. S. Huynh, D. Vincent, F. J. Perez-Pinal, M. A. Rodriguez-Licea and S. S. Williamson, "Hexagonal Geometry Coil for a WPT High-Power Fast Charging Application," *IEEE Transactions on Transportation Electrification*, vol. 5, no. 4, pp. 946-956, Dec. 2019, doi: 10.1109/TTE.2019.2941636.

[36] M. K. Kazimierczuk, Pulse-Width Modulated DC-DC Power Converters, 2 nd Ed. John Wiley and Sons, Chichester, UK, 2016.

[37] H. A. Wheeler, "Simple Inductance Formulas for Radio Coils," Proceedings of the Institute of Radio Engineers, vol. 16, no. 10, pp. 1398-1400, Oct. 1928, doi: 10.1109/JRPROC.1928.221309.

[38] G. M. Lozito, A. Laudani, A. Reatti, F. Corti, M. C. Piccirilli and L. Pugi, "Pareto Optimization of Planar Circular Coil for EV Wireless Charging," 2021 IEEE 15th International Conference on Compatibility, Power Electronics and Power Engineering (CPE-POWERENG), 2021, pp. 1-6, doi: 10.1109/CPE-POWERENG50821.2021.9501217.

[39] S. Raju, R. Wu, M. Chan and C. P. Yue, "Modeling of Mutual Coupling Between Planar Inductors in Wireless Power Applications," in *IEEE Transactions on Power Electronics*, vol. 29, no. 1, pp. 481-490, Jan. 2014, doi: 10.1109/TPEL.2013.2253334.

[40] F. Corti F, A. Reatti, A. Nepote, L. Pugi, M. Pierini, L. Paolucci, F. Grasso, E. Grasso, M. Nienhause, "A Secondary-Side Controlled Electric Vehicle Wireless Charger", *Energies*, 2020, Vol. 13, Nr. 24: pp. 6527 https://doi.org/10.3390/en13246527.

[41] W.G. Hurley, W.H. Wölfle, "Transformers and Inductors for Power Electronics: Theory, Design and Applications", 1st edition, Wiley, 2014.

[42] Jordan, Edward Conrad (1968), Electromagnetic Waves and Radiating Systems, Prentice Hall, ISBN 978-0-13-249995-8

[43] F. Ascione et al., "A closed-form equation for the local buckling moment of pultruded FRP I-beams in major-axis bending", *Composites Part B: Engineering*, 2016, Vol. 97, pp. 292-299.

[44] Su Yipin, Zhou Weijian, Chen Weiqiu, Lü Chaofeng, "On buckling of a soft incompressible electroactive hollow cylinder", *International Journal of Solids and Structures*, Volumes 97?98, 15 October 2016, Pages 400-416.

[45] Hussain I, Woo D-K, "Self-Inductance Calculation of the Archimedean Spiral Coil", Energies, 2022; 15(1):253. https://doi.org/10.3390/en15010253.

Fabio Corti received the M.S. degree in electrical and automation engineering and the PhD in industrial engineering from the University of Florence, Italy, in 2016 and 2019 respectively. He was postdoc research fellow at Consiglio Nazionale delle Ricerche (CNR) in 2020 and he is currently postdoc research fellow at the University of Perugia. His research interest includes modeling and control of DC-DC PWM and resonant converters, wireless power transfer and electric vehicle powertrain.

Alberto Reatti received the M.Sc. degree in electronics engineering from the University of Florence, Florence, Italy, in 1988, and the Ph.D. degree in electrical engineering from the University of Bologna, Bologna, Italy, in 1993. In 1992, he was an Associate Researcher with the Department of Electrical Engineering, Wright State University, USA. He has been currently an Associate Professor with the Department of Information Engineering at the University of Florence since 2000. His current research interests include high- frequency resonant, modeling and control of converters, renewable power sources and reliability of switching power converters.

Luca Pugi is currently working at the University of Florence. His research activities are focused on the mechatronics and dynamical modeling of multi-physical systems with particulat attention to mobile systems. He is author of more than 250 indexed publications and serves as reviewer and editorial board member for several scientific journals and Academic Associations, including IEEE.

Gabriele Maria Lozito was born in Rome, Italy, in 1984. He received the master degree in Electronics Engineering from the University of Roma Tre in 2010, and the Ph.D. on Softcomputing Techniques on Embedded Systems from the University of Roma Tre in 2016. He is currently Assistant Professor at the University of Florence on the main research topic of circuit modeling for renewable energy applications. His other areas of research include machine learning and optimization algorithms, embedded devices implementations and magnetic materials modeling.

Alicia Triviño-Cabrera was born in Málaga, Spain. She received the master degree in telecommunication engineering and the masters degree in computer science engineering from the University of Málaga, Málaga, in 2002 and 2008, respectively. She is currently an Associate Professor with the University of Málaga. Her thesis, which was defended, in 2007, focused on wireless networks. Part of her research work was conducted at Aston University, U.K., in 2017. Since 2011, her research has been focused on wireless power transfer. In the area of electric vehicles wireless chargers she has participated in the design of several prototypes.

Leonardo Luchetti received his bachelor's degree in electrical and telecommunications engineering at University of Florence. Since 2017 he works as mechanical designer for the automation company "Proxima s.r.l". His research interest includes wireless power transfer and finite element analysis.

Giacomo Zini received the Master's degree in electrical and automation engineering from the University of Florence, Italy, in 2022. He's currently employed in STMicroelectronics as Application Engineer, working in the sector of the smart grids. Other interests comprehend: control systems, embedded systems, machine learning and smart manufacturing.